

Using HI observations of low-mass galaxies to test ultra-light axion dark matter

James T. Garland,¹* Karen L. Masters,² Daniel Grin²

¹David A. Dunlap Department of Astronomy & Astrophysics, University of Toronto, 50 St. George Street, Toronto, ON M5S 3H4, Canada

²Departments of Physics and Astronomy, Haverford College, 370 Lancaster Avenue, Haverford, Pennsylvania 19041, USA

Accepted XXX. Received YYY; in original form ZZZ

ABSTRACT

We evaluate recent and upcoming low-redshift neutral hydrogen (HI) surveys as a cosmological probe of small scale structure with a goal of determining the survey criteria necessary to test ultra-light axion (ULA) dark matter models. Standard cold dark matter (CDM) models predict a large population of low-mass galactic halos, whereas ULA models demonstrate significant suppression in this small-scale regime, with halo mass cutoffs of 10^{12} M_\odot to 10^7 M_\odot corresponding to ULA masses of 10^{-24} eV to 10^{-20} eV , respectively. We generate random, homogeneously populated mock universes with cosmological parameters adjusted to match CDM and ULA models. We simulate observations of these mock universes with hypothetical analogs of the mass-limited ALFALFA and WALLABY HI surveys and reconstruct the corresponding HI mass function (HIMF). We find that the ALFALFA HIMF can test for the presence of ULA DM with $m_a \lesssim 10^{-21.5} \text{ eV}$, while WALLABY could reach the larger window $m_a \lesssim 10^{-20.9} \text{ eV}$. These constraints are complementary to other probes of ULA dark matter, demonstrating the utility of local Universe HI surveys in testing dark matter models.

Key words: Dark matter – cosmology: observations – galaxies: halos – galaxies: statistics – radio lines: galaxies

1 INTRODUCTION

The prevailing “cold dark matter plus cosmological constant, Λ , (Λ CDM)” cosmological model yields compelling explanations for a variety of observational measurements, from the late-time accelerated cosmic expansion, to the large-scale clustering of galaxies (Van Waerbeke et al. 2013; Alam et al. 2017; Abbott et al. 2019; DES Collaboration 2019; DES Collaboration & others. 2021), and the acoustic oscillations of the primordial plasma, probed by the cosmic microwave background (CMB) and galaxy surveys (Beutler et al. 2011; Crites et al. 2015; Louis et al. 2017; Wang et al. 2020; Planck Collaboration et al. 2020). Despite its success at large scales, Λ CDM predictions face many challenges from small scales. The over-abundance of low-mass galactic halos predicted by Λ CDM compared to those seen in observations is one such challenge, often known as the “Missing Satellites Problem” (MSP, see e.g. Papastergis et al. 2015; Bullock & Boylan-Kolchin 2017 and references therein for a more complete discussion).

The need to reconcile Λ CDM predictions with small-scale structure has fostered the exploration of alternative dark-matter (DM) models, such as self-interacting dark matter (SIDM) (Spergel & Steinhardt 2000), warm DM (Maio & Viel 2015; Bose et al. 2017; Ludlow et al. 2016), and fuzzy DM (Hu et al. 2000), all of which are motivated by considerations from high-energy particle theory (Bullock & Boylan-Kolchin 2017). These models suppress the formation of small-scale structure through DM scattering, enhanced DM velocities at early times, or macroscopic wave-like behavior, respectively

(Bullock & Boylan-Kolchin 2017). Thus, dwarf galaxies could constrain self-interacting and warm dark matter scenarios (e.g. Nadler et al. 2024). Baryon-driven processes (e.g. reionization, supernovae feedback, adiabatic contraction) could ultimately solve the MSP (Bullock & Boylan-Kolchin 2017; Elgamal et al. 2023; Widmark et al. 2023), but alternative DM candidates merit serious consideration, especially given the large number of null results from DM direct-detection experiments targeting weakly-interacting massive particle (WIMP) DM (Schumann 2019).

The ultra-light axion (ULA) is one fuzzy-DM candidate that is well motivated by the compactification of higher-index gauge fields and other considerations from string theory (Dine et al. 1981; Weinberg 1978; Nambu & Sasaki 1990; Peccei & Quinn 1977; Turner 1983). For $m_a \gtrsim 10^{-27} \text{ eV}$, the dependence of ULA energy density is the same as for matter (i.e. density, $\rho \propto (1+z)^3$) during the matter and dark-energy dominated eras. If ULAs compose some or all of the DM, they could resolve some discrepancies between the Λ CDM model and observations (Khlopov et al. 1985; Frieman et al. 1995; Arvanitaki et al. 2010; Suarez & Matos 2011; Park et al. 2012; Marsh 2016b; Hui et al. 2017). ULAs with $10^{-28} \text{ eV} \lesssim m_a \lesssim 10^{-27} \text{ eV}$ could mitigate the S_8 tension, a disagreement in the density-field variance predicted from Λ CDM fits to CMB data and that measured from galaxy-galaxy weak lensing (Lagu   et al. 2022; Rogers et al. 2023). ULA-type particles (with non-standard potentials) could also help resolve the Hubble tension (Poulin et al. 2019; Smith et al. 2020b; Agrawal et al. 2019; Lin et al. 2019; Hill et al. 2020; Smith et al. 2020a; Liu et al. 2023). In addition, ULAs show promise in remedying the MSP and other small-scale challenges for Λ CDM (Marsh & Silk 2014).

ULA simulations and halo-model calculations demonstrate the

* E-mail: james.garland@astro.utoronto.ca

presence of a cutoff in the halo mass function, predicting the suppression of the formation of low-mass galaxies, and thus improving agreement between theory and observations (Marsh & Silk 2014; Schive et al. 2014b; Veltmaat & Niemeyer 2016; Schive & Chiueh 2018; Du et al. 2017; Veltmaat et al. 2018). The galaxy scale wave-like behavior of ULAs can be thought of as a novel DM pressure (see Desjacques et al. 2018 and references therein), meaning that the competition between self-gravity and the ‘fuzziness’ of ULAs can be understood through the Jeans instability (Hu et al. 2000; Park et al. 2012). The ULA mass, m_a , thus sets a characteristic Jeans mass scale, which in turn leads to a functional relationship between m_a and a cutoff mass in the halo mass function (Marsh 2016b). Observationally testing for the existence of this small-scale cutoff could thus be a promising avenue for probing ULA DM.

Various observationally motivated constraints on the ULA model already exist. For a thorough review of progress on testing novel dark matter models with astrophysical probes, see Buckley & Peter (2018). Here we summarize some results on ULA constraints.

Observations of CMB acoustic peak height ratios are closely in agreement with the Λ CDM model, and measurements of the galaxy clustering power spectrum do not show a characteristic cutoff from ULAs at small length scales. These data thus already impose a lower limit to the axion mass of $m_a \gtrsim 10^{-25}$ eV if ULAs are to be all of the DM (Amendola & Barbieri 2006; Hložek et al. 2015; Hložek et al. 2018; Poulin et al. 2018; Laguë et al. 2021; Dentler et al. 2021). Observations of the Lyman- α forest (Armengaud et al. 2017; Iršič et al. 2017; Kobayashi et al. 2017; Nori et al. 2019; Leong et al. 2019; Rogers & Peiris 2021), stellar scattering considerations, and infall times of globular clusters around MW-dwarves (among others) critically test the ULA mass range $m_a \simeq 10^{-25}$ eV $\rightarrow 10^{-20}$ eV (see Hui et al. 2017; Bar-Or et al. 2019; Amorisco & Loeb 2018; De Martino et al. 2020 and references therein). In some cases these observations put lower limits to ULA masses, while in others, there are modest hints that ULAs improve agreement between theory and observations.

Looking to the new observational window of gravitational waves, it has been suggested that ULAs in the 10^{-16} eV $\lesssim m_a \lesssim 10^{-11}$ eV mass band could extract gravitational energy from black holes, which would have implications for gravitational-wave detection and black-hole population statistics (Arvanitaki et al. 2010). Pulsar timing arrays (PTAs) are another promising probe for the imprint of ULAs on the cosmic density field (Porayko & PPTA Collaboration 2018; Kato & Soda 2020; Hwang et al. 2024). Recent PTA evidence for a stochastic gravitational wave background imposes a powerful constraint to ULAs (Afzal et al. 2023; Antoniadis et al. 2023). Further analyses of these observations could be used to detect or rule out ULAs in the relevant mass range in coming years.

One challenge of testing cosmological models using the properties of low-mass halos is that such halos host small galaxies which can only be seen in the nearby Universe, limiting the survey volume and therefore the statistical rigour with which models can be tested with observational data. Spectroscopic HI surveys provide an interesting avenue to test for statistical measurements of the lowest-mass galaxies, because low-mass galaxies tend to be HI rich and the galaxies in an HI survey tend to be of lower masses and surface brightnesses than those in an optical survey (Huang et al. 2012).

As with all observational surveys, given a fixed observing time, spectroscopic HI surveys have to balance depth and sky coverage. Deeper surveys by necessity will cover a smaller area of sky, and therefore provide only small volumes in the nearby Universe where they are sensitive to the lowest-mass objects. The large collecting area of the Arecibo radio telescope enabled the wide area Arecibo Legacy

Fast Arecibo L-band Feed Array (ALFALFA) survey (Haynes et al. 2018) to relatively quickly survey a large sky area, and hence cover a significant volume even for local, low-mass galaxies. ALFALFA detected hundreds of galaxies with HI masses $M_{\text{HI}} < 10^8 M_{\odot}$, and even a significant number of galaxies with $M_{\text{HI}} < 10^7 M_{\odot}$ (Cannon et al. 2011). The new Five-hundred-meter Aperture Spherical radio Telescope (FAST) in China, now the largest single dish telescope in the world, also plans HI surveys. The FAST All Sky HI survey (FASHI) had its first data release earlier this year (Zhang et al. 2024) and is predicted to detect three times as many HI sources as ALFALFA (mostly due to larger sky coverage). The development of the Square Kilometer Array (SKA) and its precursors will lead to future large area spectroscopic HI surveys (e.g. WALLABY, and SKA Phase 1; Koribalski et al. 2020; Square Kilometre Array Cosmology Science Working Group 2020, respectively) which are planned to be significantly more sensitive, providing even larger numbers of HI detections, and to lower mass limits in the local Universe.

The HI Mass Function (HIMF, e.g. Zwaan et al. 2005; Hoppmann et al. 2015; Jones et al. 2018) is a statistical tool commonly used in spectroscopic HI surveys, which counts the volume number density of HI halos of a given mass. Measurements of the HIMF across a variety of survey and galaxy environments show a flattening of the low-mass slope, revealing fewer low-mass HI halos than may be found in a Λ CDM universe. Interpretation of this observation is complicated by baryonic physics which might impact the HI-mass-to-halo mass relationship, although the most extreme ULA impacts on the HIMF should still produce a clear signal.

Another promising avenue for testing the halo mass function using HI observations is via the HI velocity width function (Zwaan et al. 2010; Papastergis et al. 2011; Moorman et al. 2014). The results in Papastergis et al. (2011) using this probe clearly indicate a discrepancy with CDM models. In principle this observable probes the DM halo mass more directly than the HI mass, as the link between HI width and DM halo mass should be less impacted by scatter caused by galaxy evolution processes (see Paranjape et al. 2021 for a recent discussion of use of this as a cosmological probe). However, measuring rotation widths requires higher signal-to-noise ratio than HI masses, which may limit use at lower masses.

In this paper, we quantify the spectroscopic HI survey criteria necessary to test ULA masses in the range of $m_a = 10^{-24}$ eV to 10^{-20} eV using the HIMF of nearby Universe, low-mass galaxies. We simulate mock spectroscopic HI surveys as they would appear in a variety of ULA cosmologies by adjusting the cosmological parameters of randomly-generated mock universes. The statistics reconstructed from these mock observations allow us to simulate how the existing ALFALFA survey (Haynes et al. 2018) and upcoming WALLABY survey (Koribalski et al. 2020) would appear in a ULA cosmology, and quantify the expected reduction of low-mass halos detected relative to the predictions from a traditional CDM model. We find that using the HIMF from ALFALFA can test for the presence of ULA DM with $m_a \lesssim 10^{-21.5}$ eV, while WALLABY could reach the larger window $m_a \lesssim 10^{-20.9}$ eV.

We review the theory behind ULA as dark matter candidates in §2, and summarize the methods we use to generate mock HI surveys in §3. We show and discuss our results, in §4, and provide a summary/discussion in §5.

2 AXION COSMOLOGY

ULAs are an example of a very light scalar field, which could compose the dark matter or dark energy. Very light scalar fields are fairly

ubiquitous in string-inspired scenarios (Svrcek & Witten 2006), and may even constitute an “axiverse” of ULAs with a broad (and roughly logarithmic) distribution of masses (Arvanitaki et al. 2010). The homogeneous equation of motion for ULAs is given by Marsh (2016b, and references therein) as

$$\ddot{\phi}_0 + 3H\dot{\phi}_0 + m_a^2\phi_0 = 0, \quad (1)$$

where ϕ_0 is the homogeneous axion field, $H \equiv \dot{a}/a$ here is the conformal Hubble parameter, and a is the usual cosmological scale factor (not to be confused with m_a for the mass of the axion). At early times, the ULA energy density,

$$\rho_a = \frac{m_a^2\phi_0^2}{2} + \frac{\dot{\phi}_0^2}{2} \quad (2)$$

is roughly constant. Subsequently (when $H \ll m_a/3$), ϕ_0 begins to coherently oscillate, with the cycle averaged density scaling as $\langle \rho_a \rangle \propto a^{-3}$ (Turner 1983). This has the same scaling with a as matter. For $m_a \gtrsim 10^{-27}$ eV, the transition between these two regimes occurs after matter-radiation equality, in which case ULAs behave as matter for the bulk of cosmic structure formation and thus contribute to the DM density of the universe.

Due to the macroscopic scale of the ULA de Broglie wavelength, $\lambda_a = 1/(m_a v_a)$, where v_a denotes the axion peculiar velocity with respect to the Hubble flow, ULA linear density fluctuations grow at a suppressed rate compared with CDM inhomogeneities (causing novel interference and vortex phenomena on non-linear scales as discussed in Schive et al. 2014a, Mocz et al. 2017, Mocz et al. 2020, and Hui 2021). Averaging over oscillations in the background (homogeneous) field, ϕ_0 , and its perturbations $\delta\phi$, ULAs can be modeled as a fluid with a scale-dependent sound speed given by (Hwang & Noh 2009; Cookmeyer et al. 2020; Passaglia & Hu 2022)

$$c_s^2 \simeq \frac{k^2/(4m_a^2a^2)}{1+k^2/(4m_a^2a^2)}. \quad (3)$$

On small scales, with wavenumber $k \gg m_a a$, we thus have $c_s \rightarrow 1$, while on large scales, $c_s \rightarrow 0$, recovering CDM-like behavior. Fractional ULA density fluctuations δ_a thus obey the standard 2nd-order equation for Jeans instability (Hu et al. 2000; Park et al. 2012; Marsh 2016b) like

$$\ddot{\delta}_a + 2H\dot{\delta}_a + \left[\frac{k^2 c_s^2}{a^2} - 4\pi G \rho_a \right] \delta_a = 0, \quad (4)$$

with acoustic pressure support preventing perturbation growth for wavenumbers $k > k_J$ beyond the comoving ULA Jeans scale, where

$$k_J = (16\pi G a \rho_{a,0})^{1/4} m_a^{1/2}. \quad (5)$$

and $\rho_{a,0}$ is the present-day ULA mass density.

This modification to CDM linear growth strongly suppresses the abundance of DM halos with

$$M \lesssim M_J(z) \equiv \frac{4\pi}{3} 200 r_J^3 \rho_0(z), \quad (6)$$

where $r_J = \frac{2\pi}{k_J}$ and $\rho_0(z)$ is the mean cosmic density at redshift, z .

Precise first-principles calculations of halo abundances and correlations in ULA models require computationally expensive simulations (as in Schive et al. 2014b; Mocz et al. 2017; Veltmaat et al. 2018; Mocz et al. 2020). The halo model (Cooray & Sheth 2002) offers a sufficient tool to probe ULA models (Marsh & Silk 2014; Marsh 2016a). A variety of complications emerge, such as the choice of a filter shape for the linear density scale (Schneider et al. 2013; Marsh 2016a), the non-Markovian nature of random walks in the

ULA density field (Maggiore & Riotto 2010; Benson et al. 2013; Du et al. 2017), and the scale-dependence of the spherical density collapse threshold δ_c (Marsh 2016a). Nonetheless, it has been found that ULA halo population is well described using a mass-dependent collapse threshold (Marsh 2016a) of

$$\delta_{\text{crit}}(M, z) = G(M) \frac{\delta_{\text{crit}}^{\text{CDM}}}{D_{\text{CDM}}(z)}, \quad (7)$$

with

$$G(M) = h_F(x) \exp[a_3 x^{-a_4}] + [1 - h_F(x)] \exp[a_5 x^{-a_6}], \quad (8)$$

$$h_F(x) = \frac{1}{2} \{1 - \tanh[M_J(x - a_2)]\}, \quad (9)$$

$$x \equiv M/M_J, \quad (10)$$

and

$$M_J = a_1 \times 10^8 \left(\frac{m_a}{10^{-22} \text{ eV}} \right)^{-3/2} \left(\frac{\Omega_m h^2}{0.14} \right)^{1/4} h^{-1} \text{M}_{\odot}, \quad (11)$$

with coefficients

$$\{a_1, a_2, a_3, a_4, a_5, a_6\} = \{3.4, 1.0, 1.8, 0.5, 1.7, 0.9\}. \quad \text{Here } \delta_{\text{crit}} \simeq 1.686 \text{ is the standard CDM spherical collapse threshold and } D_{\text{CDM}}(z) \text{ is the usual CDM growth function (Carroll et al. 1992).}$$

The resulting halo population (see, e.g. Marsh 2016a) is reasonably well described by the Sheth-Tormen (ST) mass function (Sheth & Tormen 1999), which is given by

$$f(v) = A \sqrt{\frac{a}{2\pi}} v \left[(1 + av^2)^{-p} \right] \exp(-av^2/2), \quad (12)$$

where $A = 0.322$, $a = 0.707$, and $p = 0.3$, with $v \equiv \delta_{\text{crit}}/\sigma(M) = G(M)v_{\text{CDM}}$.

Use of the ST mass function assumes that the threshold for a linear overdensity at the time of halo collapse is given by the scale-independent barrier. More accurate numerical solutions for the mass function were found in Du et al. (2017). We use the ST mass function to avoid expensive solution of integral equations at many values of m_a . In future work, we will assess the impact of this approximation on our limits to ULA properties. Mass functions for a representative range of m_a values are shown in Figure 1, demonstrating the suppression of the halo mass function (HMF) compared to CDM for $M_h \ll M_J(m_a)$.

With dark-matter halo number densities in hand, we turn to the simulation of realistic HI surveys to evaluate their utility in testing ULA DM. For the simulations discussed below, we generated HMFs using 11 logarithmically spaced values in the range 10^{-25} eV $\lesssim m_a \lesssim 10^{-20}$ eV, filling in the m_a range near our ultimate lower limit with a denser grid of 20 values satisfying $10^{-22.9}$ eV $\lesssim m_a \lesssim 10^{-21.1}$ eV.

3 SIMULATION AND ANALYSIS METHODS

In this section we describe how we generate mock HI surveys in both simulated Λ CDM and axion dark matter universes.

3.1 Generating halos

We populate spherical universes 100 Mpc in radius according to the HMFs of the CDM and axion models. Each HMF model, Φ , is equidistantly binned in logarithmic mass space such that the expected number of halos in a given mass bin i is

$$N_i = \Phi(m_i)(\Delta \log M)V, \quad (13)$$

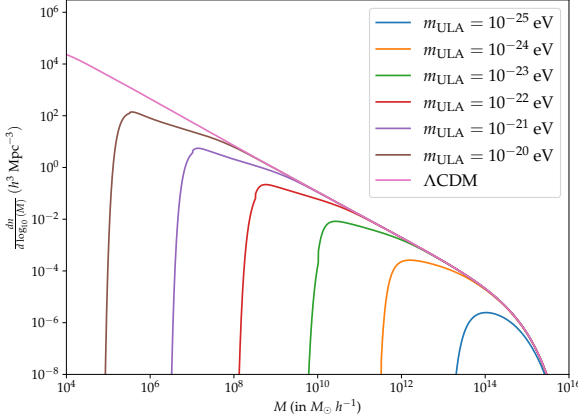


Figure 1. Halo Mass Function (HMF) for Λ CDM (pink) compared to that found for several ULA axion masses. The subtle discontinuous features appearing just below the turn-over region of our HMFs correspond to distinct features from the analytic fit to the scale-dependent δ_{crit} used in Marsh (2016a), and the linear power-spectrum obtained from AXIONCAMB.

where $\Delta \log M$ is the logarithmic distance between mass bins and V is the volume of the universe. Assuming the mass distribution of halos is Poissonian, we determine the number of halos per mass bin by sampling a Poisson distribution with an expected value determined by Equation 13.

For each halo, we select a random position within the sphere describing our mock universe and assign a randomly sampled disc inclination angle, i (from a uniform $\sin i$ distribution). While the spatial distribution of galactic halos in these universes is random, and therefore unrealistically homogeneous, the halo mass distribution is an appropriate representation of the galactic population as predicted by CDM and ULA models.

3.2 Assigning HI masses to halos

One of the most challenging steps in using HI surveys to constrain DM models is linking the HI detections to halo masses. While constraints on the baryon fraction of more massive halos ($M_h > 10^{11} M_\odot$) have been obtained from a variety of methods, complicated baryon physics, including stochastic events like supernova feedback, questions about the impact of processes during the epoch of reionization, and observational limitations, all complicate the expected baryon content of lower mass halos. Below $M_h \sim 10^8 M_\odot$, any dark matter halos that exist are not expected to contain significant baryons (Buckley & Peter 2018), so the halo mass range of particular interest is $M_h \sim 10^{8-11} M_\odot$ (probing ULA models with $m \sim 10^{-(22-24)} \text{ eV}$, see Figure 1).

In this work we use the $M_h - M_{\text{HI}}$ function in Villaescusa-Navarro et al. (2018), which is based on output from Illustris TNG (specifically TNG100; Nelson et al. 2019), a magnetohydrodynamic simulation of a $75 h^{-1} \text{ Mpc}$ box) from IllustrisTNG. They describe this using a functional form

$$M_{\text{HI}}(M_h) = M_0 \left(\frac{M_h}{M_{\min}} \right)^\alpha \exp \left(-\frac{M_{\min}}{M_h} \right)^{0.35}, \quad (14)$$

where $M_0 = (4.3 \pm 1.1) \times 10^{10} h^{-1} M_\odot$, $\alpha = 0.24 \pm 0.05$ and $M_{\min} = (2.0 \pm 0.6) \times 10^{12} h^{-1} M_\odot$. For each mock universe, we fill halos

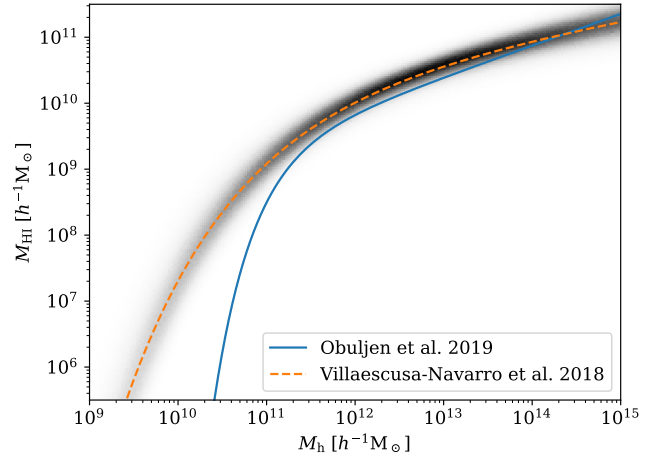


Figure 2. The M_h -to- M_{HI} relationships predicted by Villaescusa-Navarro et al. (2018) (dashed orange line) based on the TNG100 simulation. We use this relation here to fill simulated halos with HI. The greyscale heat map shows simulated galaxy HI masses corresponding to 10^7 uniformly sampled halo masses; each halo in our mock universe is assigned a corresponding HI mass assuming this model, with normally distributed uncertainties on fit parameters. Also shown is the relation measured by Obuljen et al. (2019) (solid blue line) based on ALFALFA.

of a given DM mass with HI according to this relation, selecting model parameters assuming they are normally distributed around the quoted values with the quoted uncertainties. An example result of this is shown in the greyscale heat map in Figure 2, while the Villaescusa-Navarro et al. (2018) model is shown with the dashed orange line. For a discussion of how the choice of HI-halo mass conversion might impact our final result see Section 4.2.

3.3 Mock HI observations and HIMF construction

To conduct mock observations, we determine the detectability of each halo's HI content given a set of survey sensitivity parameters. HI survey sensitivity depends both on total flux and line width, since the same amount of HI spread out over a wider velocity range will be harder to detect.

Typically the flat part of a galaxy rotation curve, as probed by the width of the HI global profile, is not at a radius which encloses all of the total halo mass. We therefore do not go directly from halo mass to rotation width using the laws of gravity, but instead assign the disc rotation velocity using the $v_{\text{flat}} - M_h$ relation found by Katz et al. (2019), namely

$$V_{\text{flat}} = 10^{-B/A} M_h^{1/A} \quad (15)$$

where they find $A = 2.902 \pm 0.138$ and $B = 5.439 \pm 0.292$ based on a fit to the SPARC dataset (a sample of 175 nearby galaxies with Spitzer data and resolved rotation curves Lelli et al. 2016), with halo profiles model as in Di Cintio et al. (2014, DC14) which they found to provide a better fit than the traditional NFW profile.

This V_{flat} is then used to obtain the “true” HI line width of $W_{\text{true}} = 2V_{\text{flat}}$. The total integrated HI flux S_{21} is largely invariant over disc inclination angle, i , since at most radii HI is optically thin, so there is minimal impact from self-absorption at 21cm (e.g. Springob et al. (2005) find self-absorption corrections to be less than 30% even in the most inclined systems), however observed line

widths are strongly dependent on inclination as only the line-of-sight velocity generates a Doppler shift, such that $W_{\text{obs}} = W_{\text{true}} \sin i$.

We use analytic approximations of survey sensitivity for both the completed Arecibo Legacy Fast Arecibo L-band Feed Array survey (ALFALFA; Haynes et al. 2018), which used the Arecibo radio telescope to survey the entire extragalactic sky accessible from Arecibo in the 21cm line at the 3' resolution provided by Arecibo, and the ongoing Widefield ASKAP L-band Legacy All-sky Blind surveY (WALLABY; Koribalski et al. 2020; Westmeier et al. 2022) which is currently running on the Australian Square Kilometer Array Pathfinder (ASKAP) with a goal of surveying 75% of the sky (the part accessible from Western Australia) in the 21cm line at 3'' resolution.

For ALFALFA, Haynes et al. (2011) cite a 90% completeness limit of

$$\log S_{21,90\%,\text{Code 1}} = \begin{cases} 0.5 \log W_{50} - 1.14, & \log W_{50} < 2.5, \\ \log W_{50} - 2.39, & \log W_{50} \geq 2.5, \end{cases} \quad (16)$$

for their “Code 1” (reliable, signal-to-noise, $S/N > 6.5$) detections, where the total HI flux, S_{21} in Jy, is linked to HI mass (in M_\odot) and the distance of the galaxy, D (in Mpc) using the standard relation of,

$$M_{\text{HI}} = (2.356 \times 10^5) D^2 S_{21}. \quad (17)$$

For WALLABY, Koribalski et al. (2020) provided an estimated 5σ M_{HI} detection limit for a source measured by a single beam as a function of line width, W^1 in km s^{-1} and distance D in Mpc as

$$M_{\text{HI}} [\text{M}_\odot] = (3901 W^{0.493}) D^2, \quad (18)$$

which corresponds to $M_{\text{HI}} = 5.3 \times 10^8 M_\odot$ at a fiducial distance of 100 Mpc and assuming typical $W = 250 \text{ km s}^{-1}$. The pilot data release for WALLABY (Westmeier et al. 2022) recently released measured sensitivity (not quoting any width dependence) of $M_{\text{HI}} = 5.2 \times 10^8 M_\odot$ at 100 Mpc, which is very comparable. In what follows we continue to use the Koribalski et al. (2020) estimate.

The effect of non-detections due to line-of-sight halo occultations should be negligible since, with HI, one can detect two halos along the same line of sight (LOS) as long as they are separated enough in redshift. If a mock galaxy with a width W_{50} (hereafter just W) and HI mass M_{HI} has a flux greater than these limits, we consider it detected in the relevant mock survey.

The output of this process is a catalogue of HI detections with halo masses, rotation widths, and HI masses. We make use of this to construct mock HI Mass Functions (HIMFs) using a $1/V_{\text{max}}$ weighting methods, where V_{max} is the maximum volume in which a detection of a given HI mass could be observed. No corrections are applied for the impact of large scale structure (LSS) or distance errors on the HIMF since our mock universes are homogeneous and we have exact distances (we refer the reader to Masters et al. 2004 for an explanation of these effects in real surveys).

3.4 Statistics of detectable differences from CDM

In order to quantify how distinguishable our simulated measured HIMFs from mock ULA dark matter universes are from fiducial Λ CDM universes, we make use of the two-sample Kolmogoroff-Smirnoff (KS) test. This is a standard statistical technique for testing

¹ It is not specified which measure of W they assume.

the likelihood that two distributions are samples of a single underlying population (i.e. that they are the same). We implement this using the SciPy Stats KS two-sample test package.²

4 RESULTS AND DISCUSSION

4.1 HIMF comparisons

We show the output HIMFs from five of our mock universes in Figure 3 corresponding to universes with dark matter comprised of a ULA with a mass $m_a = 10^{-24}, 10^{-23}, 10^{-22}, 10^{-21}, 10^{-20} \text{ eV}$ and a universe with standard CDM. Three versions of the HIMF (as both a histogram of raw number counts in the lower part of each panel, and corrected for volume in the upper part) are shown for each mock universe. We show an HIMF from an ideal survey (which detects all halos with HI mass as per the $M_{\text{HI}}-M_h$ relation (blue), as well as HIMFs generated from our mock ALFALFA and WALLABY surveys in each mock universe (blue and orange respectively).

The three measurements of each universe agree within the error bars at high masses, but deviations are seen at low mass, caused by a Malmquist bias (Malmquist 1922, 1925) type effect. Since at these masses, the majority of galaxies are below or close to the sensitivity limit of the surveys, halos with more HI than the mean trend are more likely to be detected, and since the HIMF rises (in log-space) towards lower mass halos this results in a significant turn up in the measured HIMF. This observation shows the importance of comparing mock observations of simulations to real measurements in making such comparisons (i.e. forward modelling).

We quantify the detectability of a given ULA cosmological model by considering the amount by which the observed HIMF can be seen to deviate from CDM. This deviation is calculated per mass bin in terms of $N\sigma$ as $(\Phi_{\text{obs}} - \Phi_{\text{CDM}})/\sigma_{\text{obs}}$ where Φ_{obs} and σ_{obs} are the observed HIMF and corresponding uncertainty and Φ_{CDM} is the observed CDM HIMF. The deviations from CDM as observed by our mock ALFALFA and WALLABY surveys are shown in Figure 4.

These detectable deviations from CDM in our mock universes suggest that both ALFALFA and WALLABY can constrain models with ULA masses below 10^{-22} eV , while WALLABY has the potential to constrain ULAs in the mass range up to 10^{-21} eV .

Another way to test for the deviation of axion dark matter models from CDM is via a KS test. We show this in Figure 5, which plots the median and inter-quartile ranges of p -values from a series of independent KS tests comparing the HI halo mass distributions from mock ULA universes (with particle mass as shown on the x -axis) with those from our mock Λ CDM universes in both mock ALFALFA and mock WALLABY surveys. A p -value < 0.05 (indicated by the horizontal dashed line) is typically considered to show statistically different distributions. We find that (averaged over 100 simulations) the KS test suggests statistically different HI halo mass distributions between ULA universes compared to Λ CDM for ULA masses $\log_{10}(m_a/\text{eV}) > -20.9 \pm 0.2$ for the mock WALLABY survey and $\log_{10}(m_a/\text{eV}) > -21.5 \pm 0.2$ for the mock ALFALFA survey.

4.2 Caveats and limitations

There are two ways in which our predicted constraints on the ULA mass from these mock HIMF reconstructions may be optimistic:

² https://docs.scipy.org/doc/scipy/reference/generated/scipy.stats.ks_2samp.html

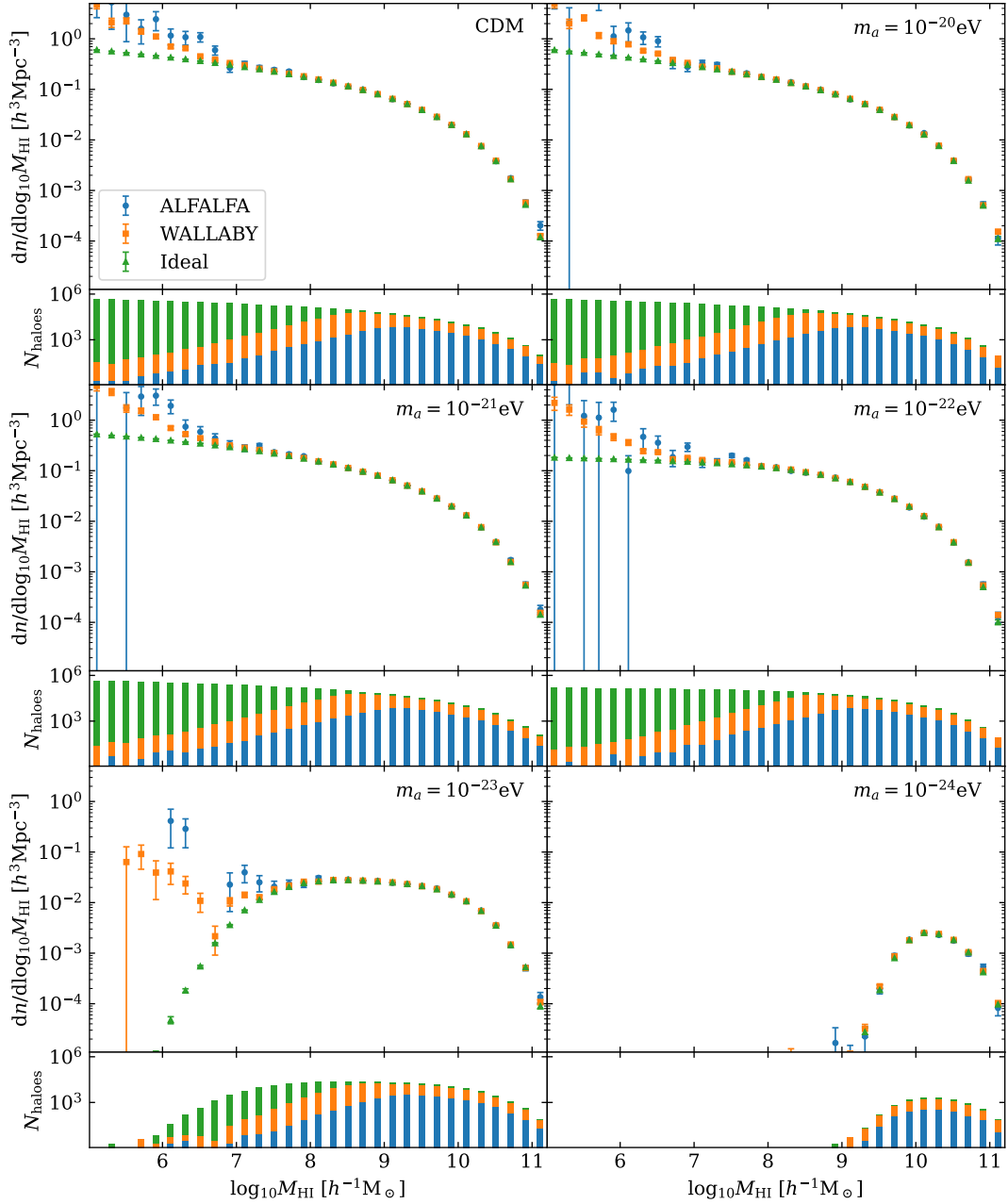


Figure 3. Mock HIMFs for a 100 Mpc survey in a Universe with dark matter that is either CDM or a ULA with $m_a = 10^{-20}$, 10^{-21} , 10^{-22} , 10^{-23} , and 10^{-24} eV (as labeled). In each of the six subplots, we show in the upper panels the observed mock ALFALFA and WALLABY mass functions (blue circles and orange squares respectively), while green triangles correspond to the same from a hypothetical ‘ideal’ survey able to observe all halos in the simulated universe (i.e. these points reflect the underlying true HIMF). Error bars account for Poisson counting error. The histograms in the lower panels show the total number of observed halos per mass bin in each survey (with the same colour scheme).

(i) We have limited our study to cosmologies in which dark matter is exclusively composed of axions. However, some mixed dark matter models that take axions to be a fraction of all dark matter display MSP-resolving halo cutoffs as well (Marsh & Silk 2014). Despite differences in other halo properties, alternative models may be subjectable to the analysis considered in this paper if they demonstrate similar HMF cutoff behavior.

(ii) The adopted $M_{\text{HI}} - M_h$ relation is based on simulated data and appears to over-represent the HI content of low-mass galaxies. There are a variety of techniques to estimate and/or measure the HI-halo

mass function. While we base this work on a predicted HI-halo mass function based on a simulation (Villaescusa-Navarro et al. 2018), it is also possible to estimate the function from real data (with significant error). For example, using ALFALFA data, Obuljen et al. (2019) fit the Schechter function,

$$M_{\text{HI}}(M_h) = M_0 \left(\frac{M_h}{M_{\min}} \right)^\alpha \exp \left(-\frac{M_{\min}}{M_h} \right), \quad (19)$$

with values of $\log_{10}(M_0/h^{-1}M_\odot) = 9.44^{+0.31}_{-0.39}$, $\log_{10}(M_{\min}/h^{-1}M_\odot) = 11.18^{+0.28}_{-0.35}$, and $\alpha = 0.48 \pm 0.08$.

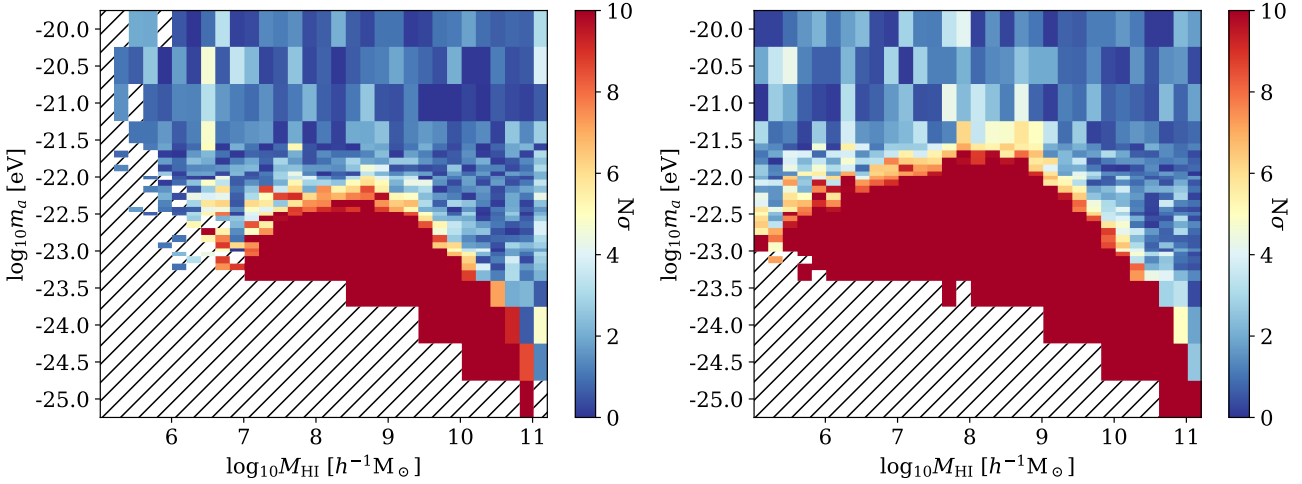


Figure 4. Deviation between ALFALFA (left) and WALLABY (right) mock HIMFs and the observed CDM HIMF in terms of observational uncertainty σ . Regions of parameter space with three or fewer HI detections in the mock surveys are shown by the slashed regions.

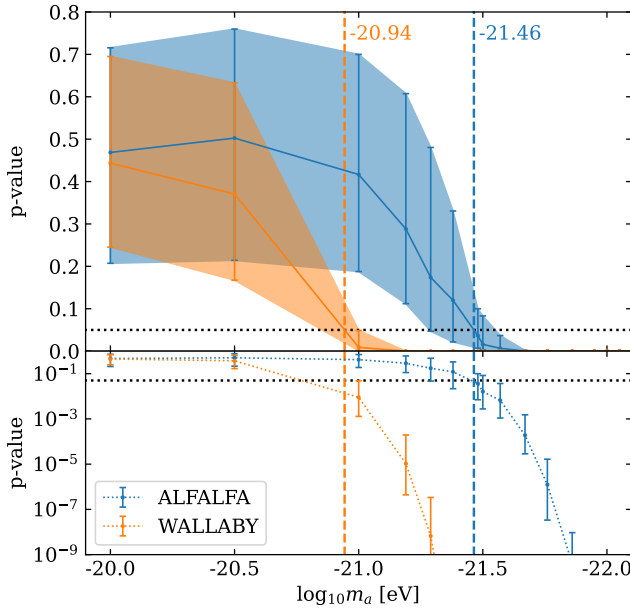


Figure 5. Linear (top) and logarithmic (bottom) display of the median and inter-quartile range (IQR) of KS-test p-values comparing mock ALFALFA (blue) and mock WALLABY (orange) surveys in ULA dark matter universes to surveys in mock Λ CDM universes. This shows the distribution of 100 sets of simulated universes in both Λ CDM and each of the axion dark matter masses. The horizontal dotted line indicates a p-value of 0.05, the typical threshold used to indicate statistically significant different distributions. Vertical dashed lines mark the inferred masses at which the surveys cross the threshold.

We show a comparison of this with the model we use in this work in Figure 2. The two lines show good agreement at higher masses, diverging from each other on low-mass scales (below about $M_h \sim 10^{11} M_\odot$, or $M_{\text{HI}} \sim 10^9 M_\odot$). An overprediction of the amount of HI in a halo mass of a given size seems to be fairly common in simulations. This discrepancy is not unexpected between observations and a simulation, since modeling gas physics, and gas phases is particularly challenging. For example, IllustrisTNG may

not account for all sources of ionizing radiation, which would impact the amount of HI able to survive in lower-mass halos. Li et al. (2022b) look at this question in several recent simulations. Thananusak & Sawangwit (2023) consider the impact this uncertainty has on the match between Λ CDM and simulated HIMFs. While our mock universes are self-consistent, our choice of $M_{\text{HI}}-M_h$ likely means our mock surveys contain a larger number of HI detections than the real ones can expect, resulting in underestimated Poisson counting errors.

While the HI–halo mass relation is often presented as a mean trend, it is well known that halos of the same mass can host a variety of HI abundances (and that this has interesting astrophysical reasons). For example, Guo et al. (2020) used a stacking analysis to directly measure the mean HI mass in galaxy groups with a range of halo masses, demonstrating this wide variation. Understanding the details of the HI bias (e.g. as in Guo et al. 2023) in filling halos is interesting both for astrophysics and the use of HI as a cosmological probe (e.g. HI intensity mapping), but beyond the scope of this paper.

4.3 Comparison with real data

Since the ALFALFA survey is already complete (Haynes et al. 2018), we can also test the ULA model against a real measured HIMF from ALFALFA. We use the HIMF published in Jones et al. (2018) and compare it to our mock ALFALFA surveys from CDM and a range of ULA universes in Figure 6. While the agreement between the real ALFALFA HIMF and our mock universes is not perfect, particularly at the highest masses, we note that this is quite likely due to uncertainty in the $M_{\text{HI}}-M_h$ relation we adopt. Indeed, the prescription of Villaescusa-Navarro et al. (2018) is known to not match the high-mass HMF in observations, and a definitive observational limit would require some modified prescription to mitigate this mismatch (Guo et al. 2020; Li et al. 2022a), accounting for any number of baryonic effects (e.g. ram-pressure stripping).

Around the knee and towards lower masses, the shape of the HIMF from ALFALFA already appears to rule out ULA (as the sole DM particle) if they have masses $m_a < 10^{-23}$ eV, however we note that dark matter comprised of ULA masses with $m_a = 10^{-22}$ eV or larger are nearly indistinguishable from CDM in this test. All of our model

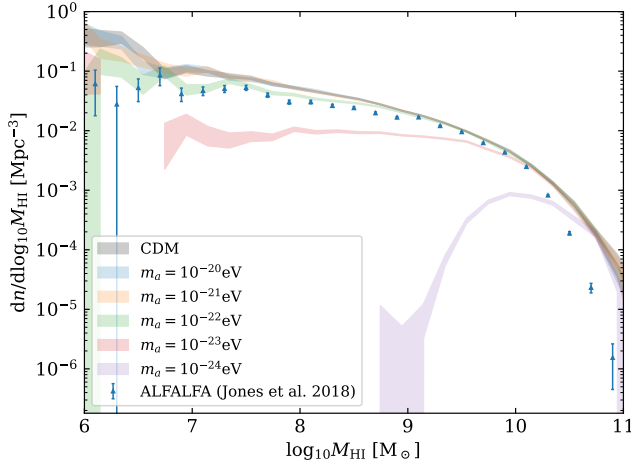


Figure 6. A set of mock ALFALFA HIMFs from universes with different models for dark matter, compared to the real ALFALFA HIMF. The mock HIMFs as observed by ALFALFA are shaded within Poissonian error range. The blue triangles correspond to the ALFALFA HIMF from Jones et al. (2018). The mock HIMFs have been corrected to be in terms of $h_{70} = 1.0$ to allow for physically meaningful comparison with real ALFALFA data. Based on this, there appears to be reasonable agreement with observed data in ALFALFA and CDM, as well as all ULA models with $m_a > 10^{-22}$ eV. ULA models with $m_a < 10^{-23}$ eV clearly do not match the data.

universes with ULA masses larger than this as well as CDM agree reasonably well with the observations from ALFALFA.

5 SUMMARY AND CONCLUSIONS

The research described in this work was motivated by a wish to explore ULA models for dark matter. This type of axion dark matter suppresses small scale structure, and might thus help to explain some of the well known inconsistencies between standard Λ CDM and observations on low mass scales.

We develop a method by which to test the potential for low-redshift large area HI surveys to constrain ULA models for dark matter via the shape of the HIMF. This involves making mock universes populated with halos from different HMFs, filling them with HI using a $M_{\text{HI}} - M_h$ relation, and then “observing” them to the sensitivity levels of recent/upcoming surveys.

We generate mock HIMFs based on universes filled with dark matter modeled as several different ULA particle masses and also CDM. We do this for both an ideal survey (i.e. detecting everything), and mock surveys designed to mimic the sensitivity of both the completed ALFALFA (Haynes et al. 2018) and ongoing WALLABY surveys. Westmeier et al. (2022) recently released WALLABY pilot data demonstrating the survey was able to reach the nominal sensitivity limits presented in Koribalski et al. (2020) (and which we used in our simulations).

We find that the HIMF measured from ALFALFA can clearly be used to detect ULAs with $m_a \leq 10^{-21.5}$ eV, while the future WALLABY survey will reach the window $m_a \leq 10^{-20.9}$ eV. This work demonstrates the promise of HIMFs measured from upcoming and/or existing large area local Universe HI surveys to place constraints on ULA models for dark matter in the range of $m_a \sim 10^{-22} - 10^{-21}$ eV.

To place our constraints in context, we show the ULA mass range probed by a variety of other astrophysical constraints in Fig. 7.

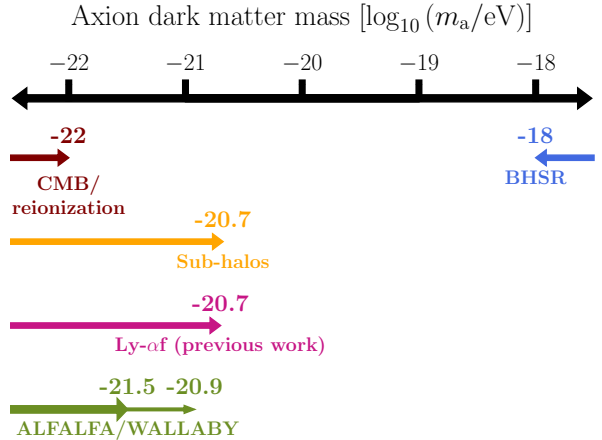


Figure 7. Mass ranges tested by a variety of astrophysical probes, including those discussed in this work.

The most robust constraints come from CMB anisotropies (including lensing and its impact on polarization) and the optical depth to reionization (Grin et al. 2019). Along with black hole spin population statistics (marked by the black hole super radiance or BHSR exclusion region), this highlights a region of interest with $10^{-22} \text{ eV} \lesssim m_a \lesssim 10^{-18} \text{ eV}$ (Grin et al. 2019). Additional (promising, but subject to considerable astrophysical uncertainty) constraints include the sub-halo mass function (as probed by strong gravitational lensing), Lyman- α forest absorption of QSO emission, and then our own work (see Grin et al. 2019; Schutz 2020; Rogers & Peiris 2021 and references therein). Our work complements considerations of using the spatial statistics of HI line-intensity mapping to test for ULA DM (Hotinli et al. 2022; Bauer et al. 2021; Kadota et al. 2021; Jones et al. 2021; Padmanabhan 2021; Kawasaki et al. 2022; Flitter & Kovetz 2022). HI data have also been applied to tests of high-mass axions in the range, $10^3 \text{ eV} \lesssim m_a \lesssim 10^5 \text{ eV}$, by considering the impact on gas cooling rates in the Leo T dwarf galaxy (Wadekar & Wang 2022).

Since the ALFALFA survey is complete, we are additionally able to compare our model to the real HIMF (we use the one published in Jones et al. 2018). This demonstrates reasonably good agreement with our mock CDM model, as well as those with ULA masses $m_a = 10^{-22}$ eV and larger, while appearing to rule out ULA dark matter with masses $m_a = 10^{-23}$ eV and smaller.

One strong motivation for considering ULAs in the mass range we explore is the *axiverse*, which posits many ultra-light fields inspired by string compactifications. As theoretical tools to model linear and non-linear structure formation in these scenarios become available (e.g. Chen & Soda 2023 and Luu et al. 2024), we look forward to exploring the impact on and constraining power of HI surveys to test these possibilities.

ACKNOWLEDGEMENTS

The authors acknowledge support from the Provost’s office at Haverford College through Summer Student Stipends. D. G. thanks K. K. Rogers for providing the original script that was modified to produce Fig. 7. D. G. acknowledges support in part by NASA ATP Grant No. 17-ATP17-0162 and the Kaufman New Initiative research grant KA2022-129518. We acknowledge useful conversations with D. J. E. Marsh, X. Du, M. Haynes, A. Lidz, J. Sippl, and R. Ghara.

The Arecibo Observatory is operated by SRI International under a cooperative agreement with the National Science Foundation (AST-1100968), and in alliance with Ana G. Méndez-Universidad Metropolitana, and the Universities Space Research Association.

The land on which the Haverford College stands is part of the ancient homeland and unceded traditional territory of the Lenape people. We pay respect to Lenape peoples, past, present, and future and their continuing presence in the homeland and throughout the Lenape diaspora.

DATA AVAILABILITY

Simulated data available on request to the authors.

REFERENCES

- Abbott T. M. C., et al., 2019, *Phys. Rev. D*, **99**, 123505
 Afzal A., et al., 2023, *Astrophys. J. Lett.*, **951**, L11
 Agrawal P., Cyr-Racine F.-Y., Pinner D., Randall L., 2019, arXiv e-prints, p. [arXiv:1904.01016](#)
 Alam S., et al., 2017, *Mon. Not. Roy. Astron. Soc.*, **470**, 2617
 Amendola L., Barbieri R., 2006, *Physics Letters B*, **642**, 192
 Amorisco N. C., Loeb A., 2018, arXiv e-prints, p. [arXiv:1808.00464](#)
 Antoniadis J., et al., 2023, arXiv e-prints, p. [arXiv:2306.16227](#)
 Armengaud E., Palanque-Delabrouille N., Yèche C., Marsh D. J. E., Baur J., 2017, *Mon. Not. Roy. Astron. Soc.*, **471**, 4606
 Arvanitaki A., Dimopoulos S., Dubovsky S., Kaloper N., March-Russell J., 2010, *Phys. Rev.*, **D81**, 123530
 Bar-Or B., Fouury J.-B., Tremaine S., 2019, *ApJ*, **871**, 28
 Bauer J. B., Marsh D. J. E., Hložek R., Padmanabhan H., Laguë A., 2021, *MNRAS*, **500**, 3162
 Benson A. J., et al., 2013, *MNRAS*, **428**, 1774
 Beutler F., et al., 2011, *Mon. Not. Roy. Astron. Soc.*, **416**, 3017
 Bose S., et al., 2017, *Mon. Not. Roy. Astron. Soc.*, **464**, 4520
 Buckley M. R., Peter A. H. G., 2018, *Phys. Rep.*, **761**, 1
 Bullock J. S., Boylan-Kolchin M., 2017, *ARA&A*, **55**, 343
 Cannon J. M., et al., 2011, *ApJ*, **739**, L22
 Carroll S. M., Press W. H., Turner E. L., 1992, *ARA&A*, **30**, 499
 Chen C.-B., Soda J., 2023, *JCAP*, **06**, 049
 Cookmeyer T., Grin D., Smith T. L., 2020, *Phys. Rev. D*, **101**, 023501
 Cooray A., Sheth R., 2002, *Phys. Rep.*, **372**, 1
 Crites A. T., et al., 2015, *Astrophys. J.*, **805**, 36
 DES Collaboration 2019, *Phys. Rev. Lett.*, **122**, 171301
 DES Collaboration others, 2021, arXiv e-prints, p. [arXiv:2105.13549](#)
 De Martino I., Broadhurst T., Henry Tye S. H., Chiueh T., Schive H.-Y., 2020, *Physics of the Dark Universe*, **28**, 100503
 Dentler M., Marsh D. J. E., Hložek R., Laguë A., Rogers K. K., Grin D., 2021, arXiv e-prints, p. [arXiv:2111.01199](#)
 Desjacques V., Kehagias A., Riotto A., 2018, *Phys. Rev. D*, **97**, 023529
 Di Cintio A., Brook C. B., Dutton A. A., Macciò A. V., Stinson G. S., Knebe A., 2014, *MNRAS*, **441**, 2986
 Dine M., Fischler W., Srednicki M., 1981, *Phys. Lett.*, **104B**, 199
 Du X., Behrens C., Niemeyer J. C., 2017, *MNRAS*, **465**, 941
 Elgamal S., Nori M., Macciò A. V., Baldi M., Waterval S., 2023, arXiv e-prints, p. [arXiv:2311.03591](#)
 Flitter J., Kovetz E. D., 2022, *Phys. Rev. D*, **106**, 063504
 Frieman J. A., Hill C. T., Stebbins A., Waga I., 1995, *Phys. Rev. Lett.*, **75**, 2077
 Grin D., Amin M. A., Gluscevic V., Hložek R., Marsh D. J. E., Poulin V., Prescod-Weinstein C., Smith T., 2019, *BAAS*, **51**, 567
 Guo H., Jones M. G., Haynes M. P., Fu J., 2020, *ApJ*, **894**, 92
 Guo H., Wang J., Jones M. G., Behroozi P., 2023, *ApJ*, **955**, 57
 Haynes M. P., et al., 2011, *AJ*, **142**, 170
 Haynes M. P., et al., 2018, *ApJ*, **861**, 49
 Hill J. C., McDonough E., Toomey M. W., Alexander S., 2020, *Phys. Rev. D*, **102**, 043507
 Hložek R., Grin D., Marsh D. J. E., Ferreira P. G., 2015, *Phys. Rev. D*, **91**, 103512
 Hložek R., Marsh D. J. E., Grin D., 2018, *MNRAS*, **476**, 3063
 Hoppmann L., Staveley-Smith L., Freudling W., Zwaan M. A., Minchin R. F., Calabretta M. R., 2015, *MNRAS*, **452**, 3726
 Hotinli S. C., Marsh D. J. E., Kamiokowski M., 2022, *Phys. Rev. D*, **106**, 043529
 Hu W., Barkana R., Gruzinov A., 2000, *Phys. Rev. Lett.*, **85**, 1158
 Huang S., Haynes M. P., Giovanelli R., Brinchmann J., 2012, *ApJ*, **756**, 113
 Hui L., 2021, *ARA&A*, **59**
 Hui L., Ostriker J. P., Tremaine S., Witten E., 2017, *Phys. Rev.*, **D95**, 043541
 Hwang J.-c., Noh H., 2009, *Phys. Lett.*, **B680**, 1
 Hwang J.-c., Jeong D., Noh H., Smarra C., 2024, *JCAP*, **02**, 014
 Iršič V., et al., 2017, *Phys. Rev.*, **D96**, 023522
 Jones M. G., Haynes M. P., Giovanelli R., Moorman C., 2018, *MNRAS*, **477**, 2
 Jones D., Palatnick S., Chen R., Beane A., Lidz A., 2021, *ApJ*, **913**, 7
 Kadota K., Sekiguchi T., Tashiro H., 2021, *Phys. Rev. D*, **103**, 023521
 Kato R., Soda J., 2020, *JCAP*, **09**, 036
 Katz H., Desmond H., McGaugh S., Lelli F., 2019, *MNRAS*, **483**, L98
 Kawasaki M., Miyazaki K., Murai K., Nakatsuka H., Sonomoto E., 2022, *J. Cosmology Astropart. Phys.*, **2022**, 066
 Khlopov M., Malomed B. A., Zel'dovich I. B., 1985, *Mon. Not. Roy. Astron. Soc.*, **215**, 575
 Kobayashi T., Murgia R., De Simone A., Iršič V., Viel M., 2017, *Phys. Rev.*, **D96**, 123514
 Koribalski B. S., et al., 2020, *Ap&SS*, **365**, 118
 Laguë A., Bond J. R., Hložek R., Rogers K. K., Marsh D. J. E., Grin D., 2021, arXiv e-prints, p. [arXiv:2104.07802](#)
 Laguë A., Bond J. R., Hložek R., Rogers K. K., Marsh D. J. E., Grin D., 2022, *JCAP*, **01**, 049
 Lelli F., McGaugh S. S., Schombert J. M., 2016, *AJ*, **152**, 157
 Leong K.-H., Schive H.-Y., Zhang U.-H., Chiueh T., 2019, *MNRAS*, **484**, 4273
 Li Z., Guo H., Mao Y., 2022a, arXiv e-prints, p. [arXiv:2207.10414](#)
 Li X., Li C., Mo H. J., Xiao T., Wang J., 2022b, *ApJ*, **941**, 48
 Lin M.-X., Benevento G., Hu W., Raveri M., 2019, *Phys. Rev. D*, **100**, 063542
 Liu G., Mu Y., Zhou Z., Xu L., 2023, arXiv e-prints, p. [arXiv:2309.02170](#)
 Louis T., et al., 2017, *JCAP*, **1706**, 031
 Ludlow A. D., Bose S., Angulo R. E., Wang L., Hellwing W. A., Navarro J. F., Cole S., Frenk C. S., 2016, *Mon. Not. Roy. Astron. Soc.*, **460**, 1214
 Luu H. N., Mocz P., Vogelsberger M., May S., Borrow J., Tye S. H. H., Broadhurst T., 2024, *Mon. Not. Roy. Astron. Soc.*, **527**, 4172
 Maggiore M., Riotto A., 2010, *ApJ*, **711**, 907
 Maio U., Viel M., 2015, *Mon. Not. Roy. Astron. Soc.*, **446**, 2760
 Malmquist K. G., 1922, Meddelanden fran Lunds Astronomiska Observatorium Serie I, **100**, 1
 Malmquist K. G., 1925, Meddelanden fran Lunds Astronomiska Observatorium Serie I, **106**, 1
 Marsh D. J. E., 2016a, arXiv e-prints, p. [arXiv:1605.05973](#)
 Marsh D. J. E., 2016b, *Phys. Rep.*, **643**, 1
 Marsh D. J. E., Silk J., 2014, *MNRAS*, **437**, 2652
 Masters K. L., Haynes M. P., Giovanelli R., 2004, *ApJ*, **607**, L115
 Mocz P., Vogelsberger M., Robles V. H., Zavala J., Boylan-Kolchin M., Fialkov A., Hernquist L., 2017, *MNRAS*, **471**, 4559
 Mocz P., et al., 2020, *MNRAS*, **494**, 2027
 Moorman C. M., Vogeley M. S., Hoyle F., Pan D. C., Haynes M. P., Giovanelli R., 2014, *MNRAS*, **444**, 3559
 Nadler E. O., Gluscevic V., Driskell T., Wechsler R. H., Moustakas L. A., Benson A., Mao Y.-Y., 2024, arXiv e-prints, p. [arXiv:2401.10318](#)
 Nambu Y., Sasaki M., 1990, *Phys. Rev.*, **D42**, 3918
 Nelson D., et al., 2019, *Computational Astrophysics and Cosmology*, **6**, 2
 Nori M., Murgia R., Iršič V., Baldi M., Viel M., 2019, *MNRAS*, **482**, 3227
 Obuljen A., Alonso D., Villaescusa-Navarro F., Yoon I., Jones M., 2019, *MNRAS*, **486**, 5124

- Padmanabhan H., 2021, *International Journal of Modern Physics D*, 30, 2130009
- Papastergis E., Martin A. M., Giovanelli R., Haynes M. P., 2011, *ApJ*, 739, 38
- Papastergis E., Giovanelli R., Haynes M. P., Shankar F., 2015, *A&A*, 574, A113
- Paranjape A., Srianand R., Choudhury T. R., Sheth R. K., 2021, MNRAS submitted, p. arXiv:2105.04570
- Park C.-G., Hwang J.-c., Noh H., 2012, *Phys. Rev. D*, 86, 083535
- Passaglia S., Hu W., 2022, arXiv e-prints, p. arXiv:2201.10238
- Peccei R. D., Quinn H. R., 1977, *Phys. Rev. Lett.*, 38, 1440
- Planck Collaboration et al., 2020, *A&A*, 641, A6
- Porayko N. K., PPTA Collaboration 2018, *Phys. Rev. D*, 98, 102002
- Poulin V., Smith T. L., Grin D., Karwal T., Kamionkowski M., 2018, *Phys. Rev. D*, 98, 083525
- Poulin V., Smith T. L., Karwal T., Kamionkowski M., 2019, *Phys. Rev. Lett.*, 122, 221301
- Rogers K. K., Peiris H. V., 2021, *Phys. Rev. Lett.*, 126, 071302
- Rogers K. K., Hložek R., Laguë A., Ivanov M. M., Philcox O. H. E., Cabass G., Akitsu K., Marsh D. J. E., 2023, *JCAP*, 06, 023
- Schive H.-Y., Chiueh T., 2018, *Mon. Not. Roy. Astron. Soc.*, 473, L36
- Schive H.-Y., Chiueh T., Broadhurst T., 2014a, *Nature Phys.*, 10, 496
- Schive H.-Y., et al., 2014b, *Phys. Rev. Lett.*, 113, 261302
- Schneider A., Smith R. E., Reed D., 2013, *MNRAS*, 433, 1573
- Schumann M., 2019, *Journal of Physics G Nuclear Physics*, 46, 103003
- Schutz K., 2020, *Phys. Rev. D*, 101, 123026
- Sheth R. K., Tormen G., 1999, *MNRAS*, 308, 119
- Smith T. L., Poulin V., Bernal J. L., Boddy K. K., Kamionkowski M., Murgia R., 2020a, arXiv e-prints, p. arXiv:2009.10740
- Smith T. L., Poulin V., Amin M. A., 2020b, *Phys. Rev. D*, 101, 063523
- Spergel D. N., Steinhardt P. J., 2000, *Phys. Rev. Lett.*, 84, 3760
- Springob C. M., Haynes M. P., Giovanelli R., Kent B. R., 2005, *ApJS*, 160, 149
- Square Kilometre Array Cosmology Science Working Group 2020, *Publ. Astron. Soc. Australia*, 37, e007
- Suarez A., Matos T., 2011, *Mon. Not. Roy. Astron. Soc.*, 416, 87
- Svrcek P., Witten E., 2006, *JHEP*, 06, 051
- Thananusak N., Sawangwit U., 2023, in *Journal of Physics Conference Series*. p. 012096, doi:10.1088/1742-6596/2431/1/012096
- Turner M. S., 1983, *Phys. Rev. D*, 28, 1243
- Van Waerbeke L., et al., 2013, *Mon. Not. Roy. Astron. Soc.*, 433, 3373
- Veltmaat J., Niemeyer J. C., 2016, *Phys. Rev.*, D94, 123523
- Veltmaat J., Niemeyer J. C., Schwabe B., 2018, *Phys. Rev.*, D98, 043509
- Villaescusa-Navarro F., et al., 2018, *ApJ*, 866, 135
- Wadekar D., Wang Z., 2022, arXiv e-prints, p. arXiv:2211.07668
- Wang Y., et al., 2020, *MNRAS*, 498, 3470
- Weinberg S., 1978, *Phys. Rev. Lett.*, 40, 223
- Westmeier T., et al., 2022, *Publ. Astron. Soc. Australia*, 39, e058
- Widmark A., Yavetz T. D., Li X., 2023, arXiv e-prints, p. arXiv:2309.00039
- Zhang C.-P., et al., 2024, *Science China Physics, Mechanics, and Astronomy*, 67, 219511
- Zwaan M. A., Meyer M. J., Staveley-Smith L., Webster R. L., 2005, *MNRAS*, 359, L30
- Zwaan M. A., Meyer M. J., Staveley-Smith L., 2010, *MNRAS*, 403, 1969

This paper has been typeset from a $\text{\TeX}/\text{\LaTeX}$ file prepared by the author.